

Fatigue of Sea Ice: A Wave-Induced Process of Rapid Self-Destruction

Erland M. Schulson, PI, Carl E. Renshaw, Co-PI,
Daniel Iliescu, Research Associate, Andrii Murdza, PhD candidate

Ice Research Laboratory
Thayer School of Engineering, Dartmouth College, Hanover, NH

22 March 2017

Abstract

New experiments reveal for the first time that the flexural strength of ice may be increased by about a factor of two upon reversed cyclic loading and that the fatigue life varies by more than two orders of magnitude.

1. Introduction

With the overall aim of better predicting failure of the sea ice cover on the Arctic Ocean and of attendant effects on the safety of ships, offshore structures and coastal communities, a study was initiated 31 March 2016 to characterize and then to understand fatigue deformation of ice. Fatigue is emerging as a significant process underlying the relatively sudden disintegration into meter-sized floes of km-sized sea ice covers (Collins et al., 2015). This report describes progress during year-1.

2. Fatigue Apparatus

We designed and then built in-house a 4-point, reversed flexing device. Figure 1 shows a computer-generated model and Figure 2 shows a photograph of the actual device now in service, made from an alloy of aluminum. The spacing between the outer and the inner pairs of cylindrical loading rods, respectively, are 254 mm and 127 mm; the rods, made from a stainless steel, are 6.4 mm in diameter. To minimize contact stresses between the loading rods and the ice, 3.2 mm wide flats were machined along the length of the rods. When in service, the wing nuts on the device (shown in Fig.2) are adjusted to just allow rod-ice contact without developing significant contact stress.

The device is attached to a model 810 MTS servo-hydraulic loading system (shown in Fig.2) housed within a cold room. In performing experiments, the hydraulic actuator of the loading system is displaced symmetrically under displacement control with respect to the neutral axis of the plate of ice. The resulting displacement of the top surface of the plate is measured using a calibrated LVDT gauge (shown in Fig. 2). The actuator's travel of the MTS loading system is load-limited in both directions (up and down) by an imposed load-limit that corresponds to the desired outer-fiber maximum stress. More specifically, loading is controlled using a FlexTest-40 controller that allows the actuator, before changing its direction of motion, to slow down momentarily as the

load approaches the prescribed limit. In other words, the actuator is displaced at the prescribed rate until the load-limit is reached at which point displacement is reversed at the same rate. The cycle period can be varied, but for our first experiments, described below, was chosen to be ~10 seconds to simulate the flexing of a natural sea ice cover. That period corresponds to a relatively low driving frequency of the order of 0.1Hz.

Reversed flexing using this device induces bending stresses, both tensile and compressive, that act in the horizontal plane of the specimen. Owing to the confining influence of the loading cylinders and to the Poisson effect, the plates are stressed biaxially: the minor stress, when calculated using isotropic elasticity and plasticity theories, is estimated to be between one-third and one-half of the major stress. For the 4-point loading device, the outer-fiber stress, σ , is computed from the relationship:

$$\sigma = \frac{3PL}{4bh^2}$$

where P denotes the applied load, L is the distance between the outer pair of loading cylinders and b and h , the width and thickness, respectively, of the specimen.

To test the performance of the device, we carried out a series of reversed flexing tests using plexiglass. A video recording is attached. The device works well. We then proceeded to perform our first experiments on the fatigue strength of ice.

3. First Experiments

3.1 Procedure:

In the interests of establishing a point of reference to which subsequent comparison will be made, we performed our first experiments on columnar-grained freshwater ice that possessed the S2 growth texture. (Within S2 ice the crystallographic c-axes of the individual columnar-shaped grains are confined more or less to the horizontal plane of the ice cover, but randomly oriented within that plane.)The only difference from first-year sea ice is the absence in freshwater ice of ~5% porosity that, within sea ice, is about half-filled with brine. Otherwise the two materials possess almost the same microstructure.

The ice was produced in the Ice Research Laboratory. Tap-water was frozen unidirectionally, top down, in a manner established by past research. The procedure produced bubble-free, S2 ice of average column diameter 5.5 ± 1.3 mm and of column length (in the direction of freezing) >50 mm. Figure 3 shows the microstructure. From such material were cut and then milled thin plates of dimensions ~13 mm in thickness (parallel to the long axis of the grains), ~75 mm in width and ~300 mm in length.

We performed two kinds of experiment, both at -10°C at an actuator displacement rate of 0.1 mm s^{-1} . The first kind was a bend test on material that had not been cycled, but bent in one direction under monotonic loading. We also performed bend tests on ice that had been cycled between load limits to determine the effect of cycling on flexural strength. The second kind of test was reversed flexing fatigue to determine the fatigue life versus stress amplitude. As will become apparent, in some experiments more than 2000 cycles were applied and in one test 7500 cycles (~20 hours) were applied without fatigue failure; in those cases, the tests were terminated by bending the ice to failure.

3.2 Flexural Strength:

For the as-grown ice loaded in an across-column direction we obtained from five tests an average flexural strength of 1.43 ± 0.20 MPa. Fracture occurred within the region between the inner loading cylinders, as shown in Figure 4. This value of flexural strength is in good agreement with values from the literature for S2 freshwater ice (Timco and Obrien, 1994) and thus lends confidence to our procedure.

Upon cycling, the flexural strength changed. Rather than decrease as one might have expected from experiments by other researchers (Nixon and Smith, 1984 and 1987; Haynes et al., 1993), the strength increased, by as much as a factor of two. This was surprising. Before considering this result, it is important to note that the ice was cycled in two ways: either (i) by cycling for about 150 times at four levels of progressively higher stress amplitude, from $\sim \pm 1.30$ MPa to $\sim \pm 2.3$ MPa, followed by a final increase to $\pm 2.40 \pm 0.20$ MPa under which the ice was cycled for up to several thousand times or (ii) by cycling under a constant stress amplitude of $\pm 1.45 \pm 0.08$ MPa. Note that the outer-fiber stresses to which the ice was subjected were generally greater than the as-grown/non-cycled flexural strength. Again, in the interests of reproducibility we made multiple measurements. Data were taken only from those tests in which fracture occurred between the inner loading cylinders; i.e., from the constant-stress region of the specimen.

The flexural strengths of the cycled ice (tests 1-10) are listed in Table 1 (tests 1-10), along with the strength of the as-grown ice (tests 11-15). Three points are noteworthy:

- (i) When grouped into two categories, cycled (tests 1-10) vs. non-cycled (tests 11-15), the results show that upon cycling in the manner described the average flexural strength increased reproducibly and significantly ($p < 0.001$) from 1.43 ± 0.20 MPa to 3.00 ± 0.44 MPa—i.e., by about a factor of two.
- (ii) When the cycled tests are considered separately, the plates that were step-cycled at progressively higher stresses for a total of 3200 ± 300 cycles (tests 8-10) failed at 3.56 ± 0.28 MPa. In comparison, plates that were cycled at constant stress amplitude for 4600 ± 1600 cycles (tests 5-7) failed at 2.81 ± 0.09 MPa. This difference is statistically significant ($p < 0.001$) and suggests that under the conditions of these experiments the cycle-induced gain in flexural strength increases with increasing stress amplitude.
- (iii) For the non-step cycled specimens that were cycled under a fixed stress of 1.45 ± 0.08 MPa, the ones that were cycled for 350 ± 38 cycles (tests 1-3) failed at 2.68 ± 0.12 MPa. In comparison, the ones that were cycled for 4600 ± 1600 cycles (tests 5-7) failed at 2.81 ± 0.09 MPa. This difference is statistically insignificant and suggests that beyond a few hundred cycles the number of cycles is not a major factor in strengthening.

In other words, these observations suggest that not only did cycling under the conditions explored increase bending strength, but that most of the gain was realized after a moderate number of cycles. Most importantly, step-cycling under increasing levels of stress amplified the gain.

Sample	Cycle stresses (MPa)	No. of cycles at max load	Total no. of cycles	Max cycle stress (MPa)	Failure stress (MPa)
1	1.58	398	398	1.58	2.75
2	1.37	358	358	1.37	2.51
3	1.41	293	293	1.41	2.80
4*	2.82	59	2193	2.82	2.82
	<i>1.69 2.03 2.26 2.54</i>				
5	1.40	4494	4494	1.40	2.96
6	1.64	2331	2331	1.64	2.74
7	1.34	7166	7166	1.34	2.75
	1.45			1.45	
8*	2.12	3214	3649	2.12	3.15
	<i>1.3 1.47 1.65 1.88</i>				
	<i>2.00</i>			2.22	
9*	2.63	2292	2951	2.63	3.64
	<i>1.29 1.50 1.88 2.31</i>			2.76	
10*	2.55	2458	3060	2.55	3.91
	<i>1.29 1.50 1.90 2.30</i>			2.69	
11		< 1	< 1		1.24
12		< 1	< 1		1.32
13		< 1	< 1		1.64
14		< 1	< 1		1.70
15		< 1	< 1		1.24

Table 1: Flexural strength (failure stress) of freshwater, S2 columnar ice at -10° C loaded across the columns, following reversed cycling at ~ 0.1 Hz. * The numbers in italics denote the stress amplitudes applied during the step-up process where the ice was cycled ~ 150 times at progressively higher stresses.

One other observation may be significant. Upon step-cycling one specimen at progressively higher stress amplitudes of ± 1.69 , ± 2.03 , ± 2.26 and ± 2.48 MPa for 490 ± 10 cycles at each level, followed by cycling at an amplitude ± 2.70 MPa for 503 cycles, we unloaded the ice and stored it overnight at -10° C for ~ 12 hours. We resumed cycling the next morning. Before a single cycle could be imparted, the specimen broke, at an outer fiber stress of 2.35 MPa; i.e., at a stress lower than the highest stress amplitude of 2.70 MPa previously applied. In other words, the over-night interruption/annealing appears to have lessened the magnitude of the cycling-induced strengthening previously imparted. Although a single observation, we wonder whether it suggests that an episode of annealing can reduce-cum-eliminate the cycling-induced increase in strength.

Deformation features: In performing the reversed flexural tests on ice that had been cycled in the manner described above, we noted some interesting deformation features. Figure 5 is a photograph of a typical example. The photograph shows plate/test-9 (Table 1) loaded in the flexural rig, prior to fracture, after having been step-cycled ~2500 times. Note the fuzzy, whitish features of grain size length (in the loading plane) distributed rather uniformly within the section of the plate between the inside support bars. The features intensified gradually during cycling rather than appearing suddenly, suggesting that they are of viscoelastic origin rather than the product of a sudden release of strain energy as in cracking. They were oriented at approximately 45° to the direction of the greater normal stress acting in the plane of the plate, as shown separately in Figure 6, suggesting that they formed through shear deformation. The whitish zones are reminiscent of similar deformation features that developed along grain boundaries within columnar-grained ice when monotonically compressed across the columns (Picu and Gupta 1995, Nickolayev and Schulson, 1995; Weiss and Schulson, 2000). We term them decohesion zones, in deference to past terminology, and take them to be evidence of localized inelastic strain imparted through grain boundary sliding. Examination of Fig. 5 and of other images like that one revealed that the zones formed on both ends of parent grains that penetrated the top and bottom surfaces of the plate; i.e., that they formed within the higher stress regions. The features extended in from both surfaces to a depth of about one-half the distance to the neutral axis of the plate; i.e., to the position within the plate where the axial stress is about one-half the outer-fiber stress. The fact that the zones extend equally inward from both the top and the bottom surfaces attests to the reversal of the loading; and their more or less uniform distribution within the central section of the plate attests to the uniform stress state that developed within that section. Decohesion zones were not detected in fractured specimens that had not been cycled (see Fig.4).

Noticeable by their absence from the two parts of plates broken after cycling were sets of microcracks, at least of the size detectable by the unaided eye. Given that upon nucleation cracks in ice are generally of grain-size dimension (Schulson and Duval, 2009), their absence implies that the first crack to nucleate propagated almost immediately, leading to the creation of the fracture surface. In other words, just as the tensile strength of more coarsely-grained aggregates is governed by the stress to nucleate the first crack (Schulson and Duval, 2009) so, too, it appears is the bend strength of the ice described here.

3.3 Fatigue Life:

Figure 7 shows the results of 21 fatigue tests during which the ice was reversibly cycled. Four sets of data are included, distinguished by color (see key in Fig.7). The coding reflects the number of ~150 cycle up-steps in outer-fiber stress amplitude before cycling to failure/fracture. Blue denotes up-steps to 1.3, 1.5, 1.9, 2.3 and finally to 2.6 MPa; orange (smaller grain size (~2 mm) to 1.3, 1.5, 1.9, 2.5 MPa; yellow, to 1.3, 1.5, 1.65, 1.88, 2.1, 2.35, 2.63 MPa; and purple, to 1.3, 1.5, 1.9, 2.6 MPa. Circles denote data that were obtained from specimens that fractured; triangles denote that fracture did not occur after the corresponding number of cycles, at which point the load was increased until the outer fibre stress, denoted by an X of the same color, was sufficient to fracture the ice. Four points are noteworthy:

(i) Pre-cycling for ~150 cycles at each of several progressively higher amplitudes of stress allows the ice to survive cyclic loading at amplitudes well above the bend strength of the material.

(ii) The fatigue life is highly variable, from as few as 5 cycles to more than 7500 cycles.

(iii) Within the scatter, it is difficult to discern any systematic trend in fatigue life.

(iv) Fracture occurred predominantly via a brittle mode; namely, transgranular cleavage.

3.4 Discussion:

The first question to address is why cycling led to strengthening in our experiments, but to weakening in those of Nixon and Smith (1984; 1987) and of Haynes et al. (1993). Our sense is that the difference is probably a reflection of the difference in experimental conditions. Temperature (-1°C vs -10°C) is probably not of major importance, for the tensile strength of ice is relatively insensitive to this parameter (Schulson and Duval, 2009). Nor is the presence (Haynes et al., 1993) versus absence (now) of contact with water likely to be important, for the fracture toughness of ice—the property that governs tensile strength of more coarsely grained material—appears not to be significantly affected by water (Sabol and Schulson, 1989). What may be important given that ice creeps at -10°C are differences in the frequency of cycling (2.8 Hz Nixon and Smith; 15-21.5 Hz Haynes et al.; vs ~ 0.1 Hz here). The other important difference—and this we think is key—is difference in the magnitude of the stresses. Calculations described in the Appendix estimate for the floating plate of the work by Haynes et al. (1993) a maximum mean stress of around 0.8 MPa and a stress amplitude of about 0.3 MPa, while in the work of Nixon and Smith (1984; 1987) the outer-fiber stress level was lower than 0.7 MPa (our estimate from the data they present). These levels compare to a stress amplitude in our work that stepped up from 1.3 to 2.6 MPa. Stresses of that magnitude are sufficient to activate the grain boundary decohesion that we observed, for decohesion requires stresses around 0.9-1.1 MPa (Picu and Gupta, 1995)—lower than the stresses we applied by higher than the stresses applied by earlier investigators.

How do decohesions allow cyclic strengthening? We imagine that reversed cycling and the attendant reversal of the direction of grain boundary sliding lessens the effectiveness of internal stress concentrators located at grain boundaries, such as facets and ledges of the kind observed by Liu and Baker (1995), possibly through the development of a dislocation substructure and an accompanying back stress that is heightened owing to the small number (two) of independent slip systems in ice. As a result, the applied stress must increase to nucleate the crack that eventually propagates, thus raising the flexural strength. Annealing would reduce the back stress by eliminating/rearranging the substructure, thereby reducing/eliminating the strengthening.

On fatigue life, it is perhaps not surprising that this property is characterized by a high degree of scatter, given the brittle character of fracture. Clearly, more work is needed to establish a pattern.

4. Next Steps

Now that experimental procedures have been developed and that a first set of results has been obtained, our plan for year-2 is to introduce S2 sea ice into the program. Questions to be answered include:

- Does the flexural strength of sea ice mimic the flexural strength of freshwater ice and thus increase upon step-up cycling? If not, why not?
- Is the fatigue life of sea ice less scattered than that of freshwater ice?
- Once a pattern has been established, does fatigue life obey Basquin's law?

At the same time, we plan to continue to establish a reference fatigue curve using freshwater ice.

References

- Bernshteyn S (1929) The railway ice crossing. *Trudy Nauchono-Tekhnicheskogo Komiteta rondnogo Komissariata Putei Soobshcheniya*, **84**, 36-82
- Collins CO, Rogers WE et al. (2015) In situ measurements of an energetic wave event in the Arctic marginal ice zone. *Geophys. Res. Letts.*, **42**, doi:10.1002/2015GL063063
- Haynes FD, Kerr AD and Martinson CR (1993) Effect of fatigue on the bearing capacity of floating ice sheets. *Cold Reg. Sci. Technol.*, **21**(3), 257-263 (dx.doi.org/10.1016/0165-232X(93)90069-K)
- Kerr AD (1976) The bearing capacity of floating ice plates subjected to static or quasi-static loads. *J. Glac.*, **17**(76), 229-268
- Liu F, Baker I and Dudley M (1995) Dislocation-grain boundary interactions in ice crystals. *Phil. Mag. A*, **71**, 15-42
- Nickolayev OY and Schulson EM (1995) Grain-boundary sliding and across-column cracking in columnar ice. *Phil. Mag. Ltrs.*, **72**(2), 93-97 (dx.doi.org/10.1080/09500839508241619)
- Nixon WA and Smith RA (1984) Preliminary results on the fatigue behavior of polycrystalline freshwater ice. *Cold Reg. Sci. Technol.*, **9**, 267-269
- Picu RC and Gupta V (1995) Observations of crack nucleation in columnar ice due to grain boundary sliding. *Acta Mater.*, **43**(10), 3791-3797 (http://dx.doi.org/10.1016/0956-7151(95)90163-90)
- Sabol SA and Schulson EM (1989) The fracture toughness of ice in contact with salt water. *J. Glac.*, **35**(120), 191-192 (doi: 10.1017/S0022143000004482)
- Schulson EM and Duval P (2009) *Creep and fracture of ice*. Cambridge University Press, Cambridge
- Timco GW and O'Brien S (1994). Flexural strength equation for sea ice. *Cold Reg. Sci. Technol.*, **22**(3), 295-298 (dx.doi.org/10.1016/0165-232X(94)90006-X)
- Weiss J and Schulson EM (2000) Grain-boundary sliding and crack nucleation in ice. *Phil. Mag. A*, **80**(2), 279-300 (dx.doi.org/10.1080/01418610008212053)

Appendix

We estimated the bending stress within the floating ice plates of Haynes and others (1993) as follows: From a load P uniformly distributed over a circular area πa^2 on an infinite plate of ice of thickness h and of Young's modulus E and Poisson's ratio ν floating on water of density ρ , the bending stress is given by (Bernshteyn, 1929; see also Kerr, 1976):

$$\sigma = \frac{3(1+\nu)C(\alpha)P}{h^2} \quad (\text{A1})$$

where $C(\alpha)$ is a dimensionless parameter that decreases as α increases;

$$\alpha = a/l \quad , \quad (\text{A2})$$

$$l = (D/\rho)^{1/4} \quad , \quad (\text{A3})$$

$$D = Eh^3/12(1-\nu^2) \quad . \quad (\text{A4})$$

From the experiments of Haynes et al. (1993), $a=0.08$ m, $h=0.03$ m, $E=5\times 10^8$ kg m⁻² (or 5 GPa), $\nu=0.33$, $\rho=10^3$ kg m⁻³ which give $D=1250$ kg m, $l=1.06$ m and $\alpha=0.08$; correspondingly, from Fig. 3 of Kerr (1976) $C(\alpha)=0.45$. Thus for a static load of $P=471$ N and an oscillating load amplitude of 176 N (Haynes et al., 1993) we estimated from the analytical model the static or mean stress to be 0.84 MPa and the stress amplitude to be around 0.32 MPa.

We also performed a numerical analysis, which led to similar estimates, of 0.77 MPa for mean stress and 0.29 MPa for stress amplitude. For the numerical calculations ice was considered to be an isotropic linear elastic material and the domain size was taken to be ten times larger than the area over which distributed load was applied. This is also in accordance with the characteristic length in Haynes and others, (1993). Vertical lateral boundaries of the domain were fixed. The bottom surface, which had contact with water, was assumed to be a damping surface with a force proportional to displacement that acts in opposite direction. We used in the analysis the equilibrium equation $\nabla\sigma + F_v = 0$, where F_v is the body force.

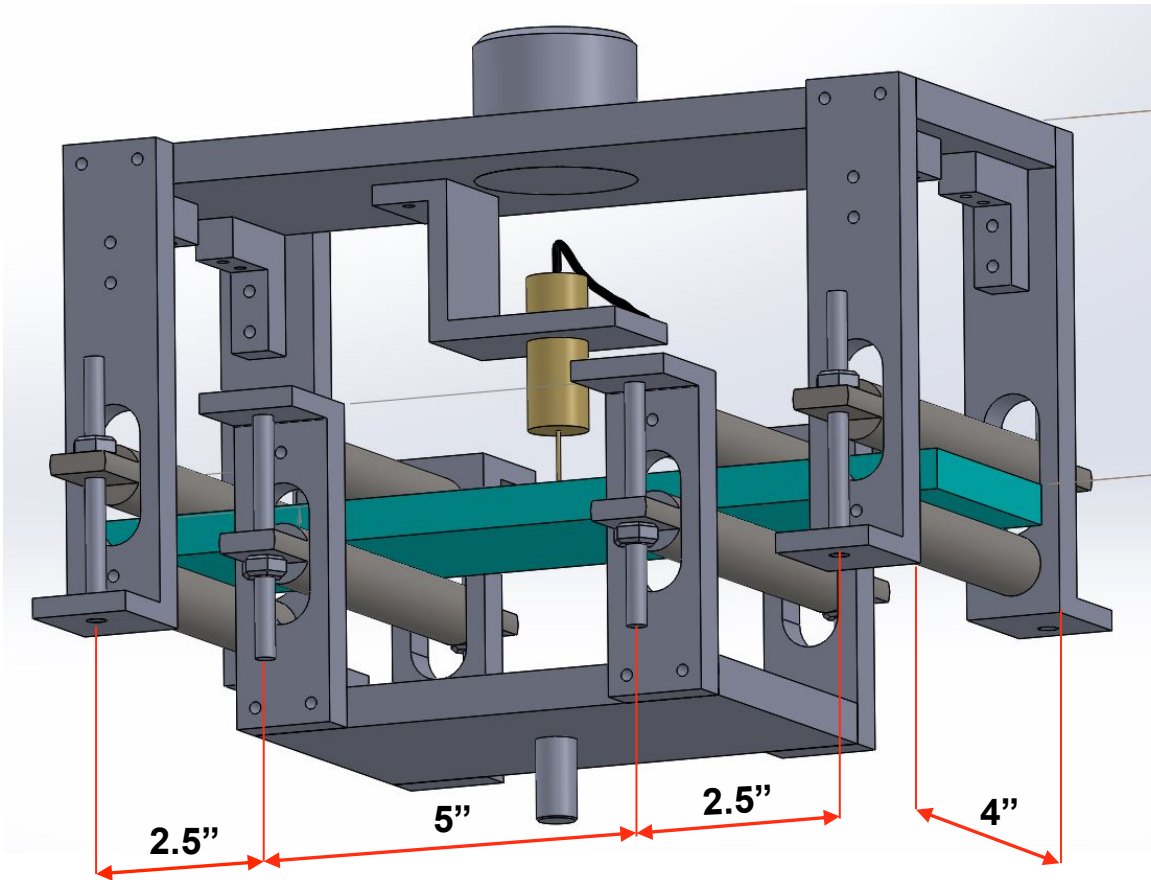


Figure 1: Computer-generated model of the flexing device.

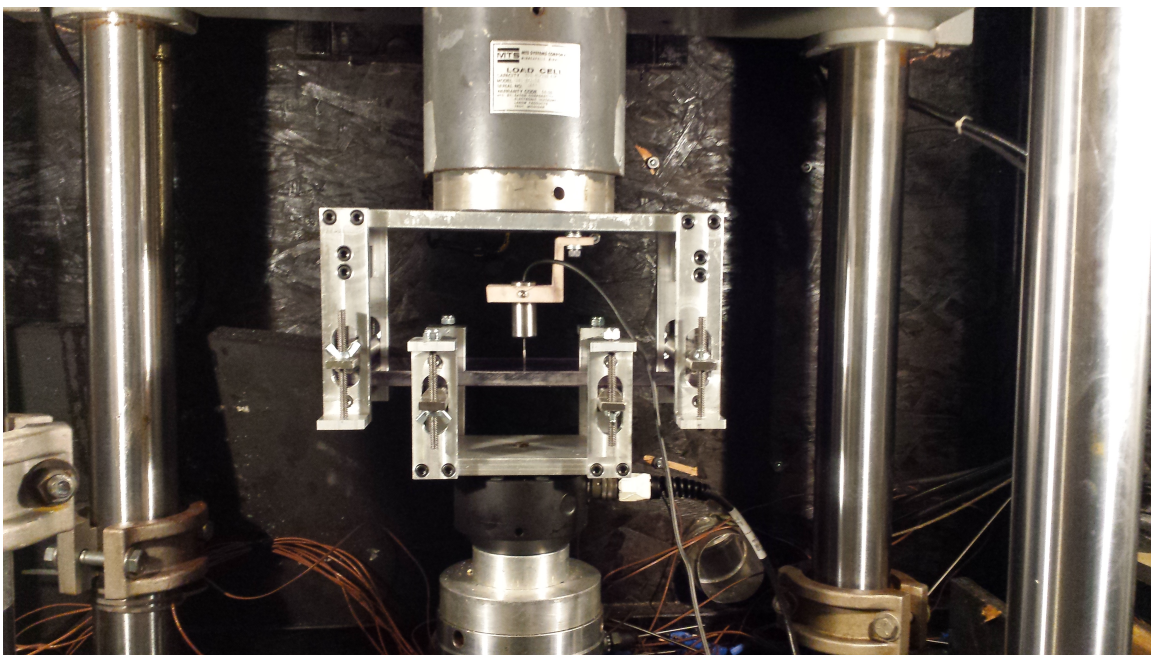


Figure 2: Photograph of 4-point, reversed-loading, flexing device.



Figure 3: Photograph of a vertically-oriented thin-section (~1mm) of columnar-grained, freshwater ice as viewed between crossed-polarized filters.

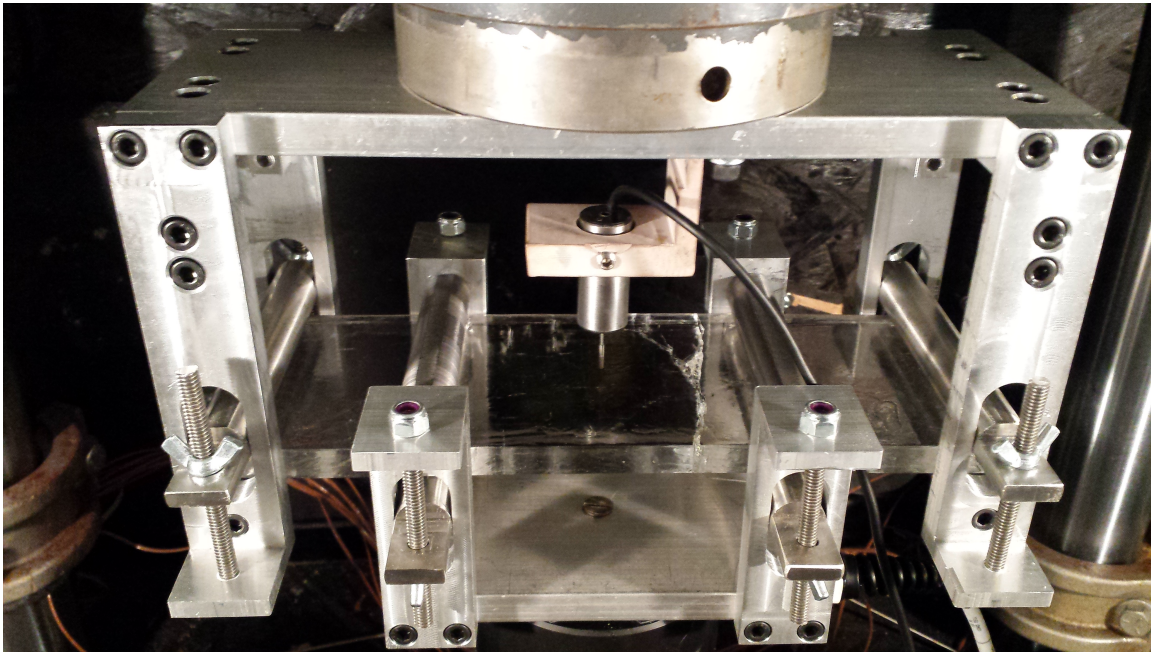


Figure 4: Photograph showing the fracture path within a plate of an as-grown/non-cycled S2 freshwater ice that had been flexed to failure, showing the fracture path between the inner loading cylinders. The long axis of the columnar-shaped grains is perpendicular to the upper and lower surfaces of the plate.

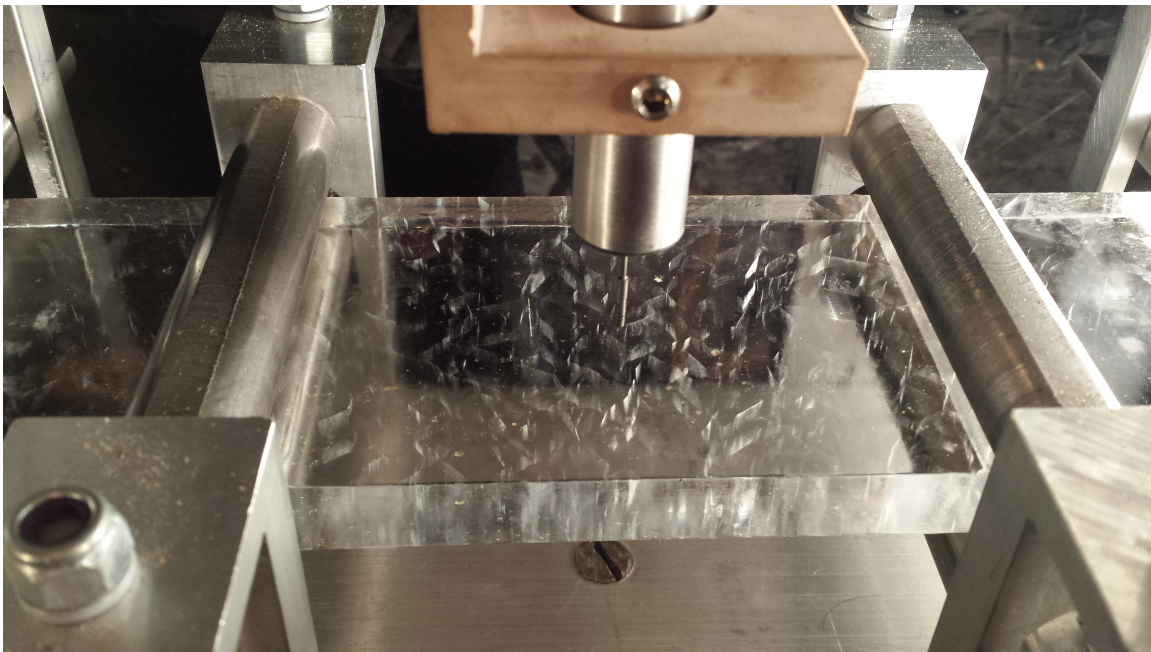


Figure 5: Photograph showing a test specimen in the reversed-cyclic loading frame, after cycling ~ 2500 times at a displacement rate of 0.1 mm s^{-1} at -10° C . Note the whitish features located at grain boundaries, stemming equally from the upper and lower surfaces (e.g., a-a and b-b). The features are termed decohesion zones.

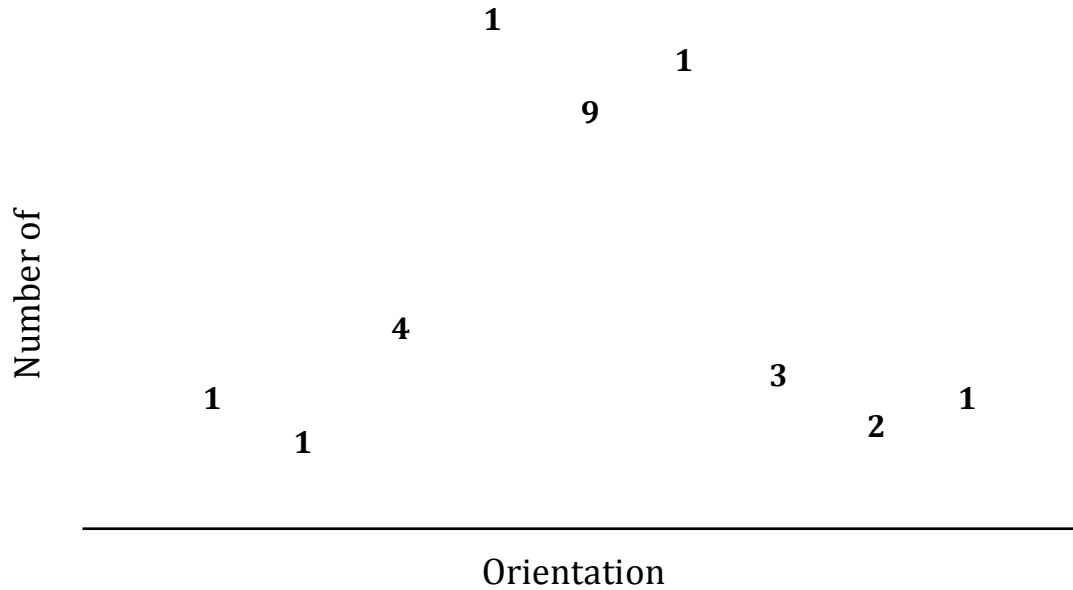


Figure 6: Histogram plot showing number of occurrences in each bin across the measured angle distribution. In this case, the angles made by the decohered grain boundaries with respect to the longitudinal axis of the specimen are binned and the number of decohered boundaries in each bin represents the number of occurrences. The normality test indicates that the distribution is likely normal with a mean of about 40° and a standard distribution of about 16° .

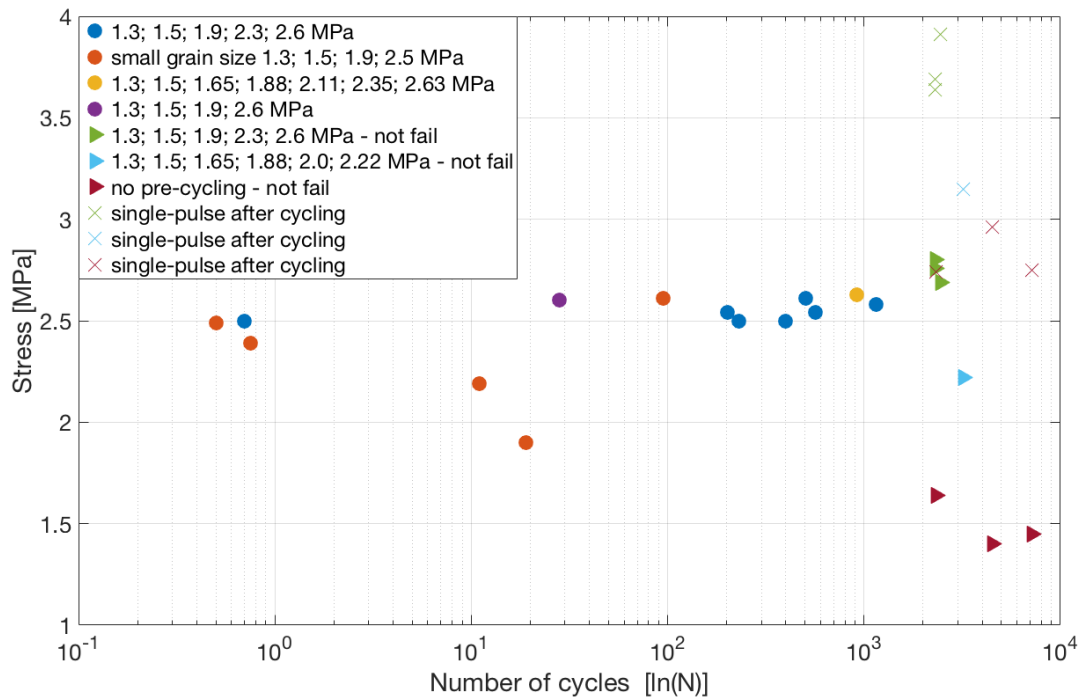


Figure 7: Plot of stress amplitude versus number of cycles to either fatigue fracture (circles) or to bend fracture (X's) after cycling for 2500-7500 cycles without fatigue failure (triangles color-coded with the X's).